# An Experimental Study of Insufficient Free Board Effect on Fixed-Roof Cylindrical Tank Seismic Loads

**Mojtaba Moosapoor[1], Mohammad Mehdi Yousefi[2], and Mohammad Ali Goudarzi[3*]**

1. Ph.D. Candidate, International Institute of Earthquake Engineering and Seismology (IIEES), Tehran, Iran
2. Ph.D. Student, Babol Noshirvani University of Technology (BUT), Babol, Iran
3. Associate Professor of Structural Engineering Research Center, International Institute of Earthquake Engineering and Seismology (IIEES), Tehran, Iran,
*Corresponding Author; email: goudarzi.ma@gmail.com

**Received:** 30/07/2019
**Accepted:** 16/05/2020

## ABSTRACT

*Cylindrical tanks are fundamental structures used for the storage of liquids. Sloshing caused by earthquakes in tanks without enough freeboard leads to a liquid impact on the roof of tanks. This study aims to explore the base shear variation due to insufficient freeboard using experimental and numerical methods. The experimental tests are performed using a cylindrical liquid tank excited by various harmonic loads. The impact of some parameters such as the water height to tank radius ratio and freeboard on base shear force are investigated by conducting 90 tests. Impulsive and convective masses for simplified mass-spring are modified in numerical models so that experimental and numerical base shear results are consistent. Finally, a simple analytical solution to estimate the reduction of convective mass due to insufficient freeboard is suggested and validated using experimental results.*

**Keywords:**
Liquid Tanks; Strengthening; Seismic Behavior; Numerical Methods

## 1. Introduction

Cylindrical storage tanks are prevalent structures utilized globally to store water, chemicals, and petroleum products. Their safety and durability are really essential because there can be severe consequences even for minimal failure. Earthquake is one of the most severe natural hazards damaging major industrial facilities. Immediately after the damaging earthquakes, water supplies are vital not only to deal with possible subsequent fires but also to prevent disease epidemics. Therefore, in addition to tanks economic cost, the seismic performance of liquid storage tanks is of particular significance owing to the need to remain operational after a major earthquake. However, dynamic response of the steel cylindrical liquid storage tank strongly relies on the interaction between the fluid and structure including the sloshing of the liquid and the vibration of the tank structure. This emphasizes the required clarification for the tank structure's safety.

The vertical cylindrical tank is the most suitable types of container. Damage to fluid storage tanks caused by previous earthquakes has inspired several experimental and analytical studies on vertical cylindrical tank seismic reaction. In order to predict seismic tanks responses such as base shear, overturning moment and maximum sloshing wave height (MSWH), some simplified Mass-Spring-

Models (MSMs) have been proposed. The sloshing phenomenon can cause adverse and destructive effects in liquid storage tanks subjected to seismic loads. For instance, the failure of the floating roof and the fire of oil storage tanks due to the impact of liquid waves were frequently observed [1]. MSWHs are used for calculating sufficient free-board between the surface of liquid and tank roof to prevent the impact of sloshing waves on the roof [2].

Since the early 1930s, several studies have been conducted on the seismic reaction of rigid cylindrical liquid storage tanks. In order to calculate the seismic reaction of liquid storage tanks, a simple MSM was proposed by Housner [3-4] and gained further widespread popularity after minimal adjustments for rectangular and cylindrical tank analyses. The simplified MSM proposed for a stiff tank was comprised of two single-degree-of-freedom (SDOF) systems; one SDOF system accounting for the movement of the tank-liquid structure where a portion of the stored fluid is rigidly connected to the reservoir wall known as an impulsive mode, and the other SDOF system takes into account the sloshing fluid effect on the reservoir wall known as a convective mode [5]. Regarding the flexibility of steel tanks walls, some scientists showed that the hydrodynamic stress in flexible liquid storage tanks was considerably increased compared to the solid tanks (Veletsos and Yang [6]; Haroun and Housner [7]). For instance, Veletsos [8] introduced a method assuming that the seismic loading reservoir acts as a cantilevered beam. They also add one convective mass and spring to the Housner's model to consider the effect of higher modes. Malhotra et al. [9] used one convective mode to modify the properties of the simplified MSM proposed by Veletsos and Yang [6]. Moreover, Goudarzi and Sabbagh-Yazdi [10] examined the reliability of the results of the modified MSM developed by Malholtra et al. [9] for the design of liquid storage tanks using a finite element model (FEM). They found out the results calculated from the FEM analysis of time history show good agreements with the simplified MSM for most cases.

The MSM based on linear theory has been widely used by numerous researchers and well-known design standards to measure the seismic design parameters (e.g. free surface displacement, base shear, and overturning moment) for liquid storage tanks. For evaluating small amplitude motions in tanks, analytical solutions based on linear wave theory are very useful. Abramson [11] used a linear theory to simulate the sloshing of small amplitude in a container. Furthermore, Chen and Chiang [12] used the Euler equation to evaluate the sloshing flow caused by the wave in a rigid floating tank. Wu et al. [13] provided an analytical solution for linear Navier - Stokes equations with a linear free-surface condition for sloshing waves. Goudarzi and Sabbagh-Yazdi [14] investigated the non-linear behavior of sloshing in rectangular tanks using numerical and experimental methods. They concluded that the non-linear effects resulted in larger sloshing wave height than the linear condition only in broad tanks. Kabiri et al. [15] also performed an elaborate investigation on sloshing wave impact force (SWIF) due to insufficient freeboard in rectangular tanks using both numerical and experimental methods. They performed several shaking table tests on small-scale tanks to validate their numerical models and then studied the SWIF in full-scale tanks using numerical simulation. They showed that the simplified methods suggested by standard codes (e.g. ACI) for calculating SWI, considerably under-estimate the sloshing force.

In addition to analytical researches, De Angelis et al. [16] conducted an experimental investigation on the seismic response of a floating roof-equipped storage tank in a number of shaking table experiments. The experiments did not, however, consider the level of the contained fluid. Zhang et al. [17] performed shaking table tests on a steel storage tank to investigate the performance of friction pendulum bearings but they also did not considered the contained fluid height. Burkacki and Jankowski [18] conducted a shaking table test on a scaled 1:33.33 model and found that the height of the liquid inside a container had a significant impact on the dynamic response and therefore is an important factor to consider in structural analysis. Bae and Park [19] have provided the outcomes of shaking table tests to examine the impacts of the fixed roof and the additional mass at the top of the tank on dynamic behavior of the tank. Park et al. [20] also researched oval-type and beam-type vibration methods using shaking table experiments at various water levels on a cylindrical fixed-roof steel tank.

In fixed-roof tanks, sufficient freeboard distance is necessary to avoid the impact of the wave on the tank roof and liquid sloshing during the earthquake. Sloshing can cause a significant hydrodynamic impact on the roof of the storage tank if the free-board is not adequately taken into account. Hence, it is difficult to assess the maximum sloshing wave height for various situations and consequently the sufficient freeboard which is not even always feasible. The insufficient freeboard has two major effects on tanks: Firstly, this phenomenon causes a huge upward force on the roof of the tanks owing to the sloshing pressure. Several researchers had investigated this phenomenon, for instance Milgram [21] studied pressure distribution on a liquid tank roof by carrying out a series of experiments in a pool-type reactor vessel. Minowa [22] and Minowa et al. [23] conducted a sequence of shaking table experiments on a rectangular tank to assess roof impact pressure, natural frequencies, and bulging vibration modes. Their outcomes indicated the risk of serious damage owing to the sloshing impact. Goudarzi et al. [24] studied sloshing-induced effect through experimental research and proposed an analytical method to evaluate the maximum impact force on tank roofs. Secondly, it may increase impulsive and decrease convective masses. Subsequently, this increases base shear force due to constraining performance of the roof. It should be highlighted that despite the significant effect of the latter feature, so far neither numerical modeling nor experimental studies have been performed to estimate its impact on shear-base forces. In this regard, Malhotra [25-26] introduced a simple practical procedure in order to measure sloshing pressure in case of insufficient freeboard. According to this study, for zero free board, the entire fluid mass moves along with tank and acts like an impulsive mass. Consequently, as the convective mass reduces linearly towards zero, the impulsive mass increases linearly towards the total mass of liquid as a function of actual-to-required free board ratio. The approach is mostly proposed for practical purposes because it is rely on too simplified assumptions and we believe further investigation is required to evaluate the accuracy of this method.

The primary goal of this study is to investigate hydrodynamic forces redistribution and discuss the variation of impulsive and convective masses with insufficient freeboard in cylindrical vertical storage tanks.

In this study, we start our presentation with a description of the mass spring model and we then explain the series of comprehensive experiments undertaken on a small-scaled cylindrical tank excited by various harmonic time histories. Then, we proposed a theoretical equation to estimate impulsive and convective masses for tanks with insufficient freeboard using the results calculated from experimental tests under liquid sloshing effect during harmonic excitation. Using the resulting impulsive and convective masses, we calculated base-shear forces for numerous experimental cases, and then compared them with the experimental results.

In addition, this paper discusses the influence of various loading frequencies on base shear values after various freeboards using the modified masses. This work was performed on five cylindrical fix roof tanks having different height of water-to-radius of tanks ratios. Finally, attempts are made to scrutinize the shear waves as functions of water height and loading frequency parameters for two tanks with different H/R ratios.

## 2. Simplified Mass Spring Model (MSM)

Simplified MSM was initially introduced by Housner [3-5]. After that, Veletsos and Yang [6] improved Housner's model by considering the effects of tanks wall flexibility on the pressure distribution of liquids and its corresponding forces on the tank structure using an analytical model. Following that Malhotra [9] enhanced Veletsos and Yang [6] model by: 1) adding the higher impulsive and convective modal mass to their first modes, 2) generalizing the formula for the impulsive period to be applied to steel and concrete tanks of different wall thicknesses, and 3) modifying impulsive and convective heights.

The simple MSM is shown in Figure (1). As shown in this figure, impulsive mass, denoted as $m_i$, and convective mass, denoted as $m_c$ are both connected to tanks wall with springs. Values of these masses, their natural periods as well as their heights ($h_i$ and hc in Figure 1) are presented by Malhotra [9] for different H/R ratios. Although the

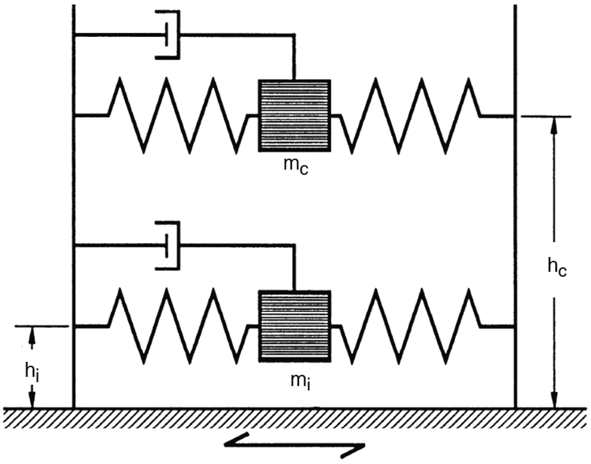


**Figure 1.** Simplified MSM [9].

convective mass contribution is small for slender tanks, for broad tanks, it can be more than 50% of the total liquid mass.

One of the fundamental assumptions of the simple MSM is the free movement of the liquid surface, so that in presence of the fixed-roof, sufficient freeboard must be deemed to avoid the impact of waves on the tank roof. An insufficient freeboard in tanks affects the distribution of hydrodynamic forces and subsequently changes the impulsive and convective mass portions which results in a change in the base shear force.

If the freeboard falls to zero, the liquid cannot generate any waves and therefore, the convective mass tends to diminish. As to before-mentioned fact, Malhotra [25-26] proposed simple relationships (Equations 1, 2) to modify and recalculate the impulsive and convective masses, particularly for further use in engineering practices. He assumed convective mass decreases linearly from mc for sufficient freeboard to zero for zero freeboard and consequently, the impulsive mass increases linearly from $m_i$ towards the total mass of liquid.

$$\overline{m_i} = \begin{cases} m_i + m_c \times \left(1 - \dfrac{d_f}{d}\right) & \text{for } d_f < d \\ m_i & \text{for } d_f \ge d \end{cases} \quad (1)$$

$$\overline{m_c} = \begin{cases} m_c \times \dfrac{d_f}{d} & \text{for } d_f < d \\ m_c & \text{for } d_f \ge d \end{cases} \quad (2)$$

In Equations (1) and (2), $m_i$ and $m_c$ are the impulsive and convective masses respectively in case of sufficient freeboard, computed through commonly used standards. $(\overline{m_i})$ and $(\overline{m_c})$ are the modified impulsive and convective masses, respectively; and $d$ and $d_f$ are actual and required freeboard, respectively. It should be highlighted that in case of inadequate freeboard, $(\overline{m_i})$ and $(\overline{m_c})$ should be used instead of $m_i$ and $m_c$.

In tanks having short freeboard, seismic design forces (e.g. base shear) may significantly alter gradually due to the sloshing impact to the roof leading to changes in the dynamic force values. It is worth mentioning that except the simple equations developed by Malhotra [25-26], this feature has not been studied in detail, and more importantly it has not been embedded in any design codes and standards. Providing a detailed investigation of this phenomenon is of particular importance.

## 3. Experimental Study

In present study, the experimental measurement was considered as the principal technique to study the influence of the insufficient freeboard on seismic design forces for cylindrical tanks subjected to various harmonic time histories. For this purpose, a tank of 1 m diameter and 1.2 m height made of Plexiglas plates with 2 cm thickness was used to perform experimental tests (Figure 2). Figure (2) shows the schematic (right panels) and real (left panels) pictures of the experimental setup used in present study.

As indicated in Figure (2), the under-studied storage tank (Figure 2-a) was connected rigidly to the horizontal steel frame placed on four bearings (Figure 2-c) to prevent any transferring forces from the surface of the shaking table (Figure 2-b) to the tanks bottom. This enabled us to accurately measure the base shear forces under the harmonic loads.

In order to measure the total shear force, two horizontal force transducers (Figure 2-e) were utilized while attached to a solid supporting steel structure (Figure 2-f) to transfer the total movement of the shaking table to the storage tank. The details of the structure and transducers are indicated in Figure (2). For adjusting the height of the roof, four stud bolts are attached to the roof, which allowed us to shift the roof at various heights.

In order to investigate the water height effect, four cases were considered as follows: 25, 50, 75, and 95 cm water depths that represent H/R ratios of 0.5, 1, 1.5, and 1.9, respectively.

As indicated in Table (1), each H/R case is presented as functions of harmonic loading and freeboard. Harmonic loadings are introduced by two parameters namely frequency and amplitude of the applied loads. The first and second load case represent a frequency lower than and equal to the resonant frequency of convective mode. The last two loadings (load cases 3 and 4) represent frequencies higher than the resonant frequency of convective mode. The details of all loading categories are shown in the first row of Table (1). Furthermore, for each load case, four to seven different freeboard heights were considered for further investigation.

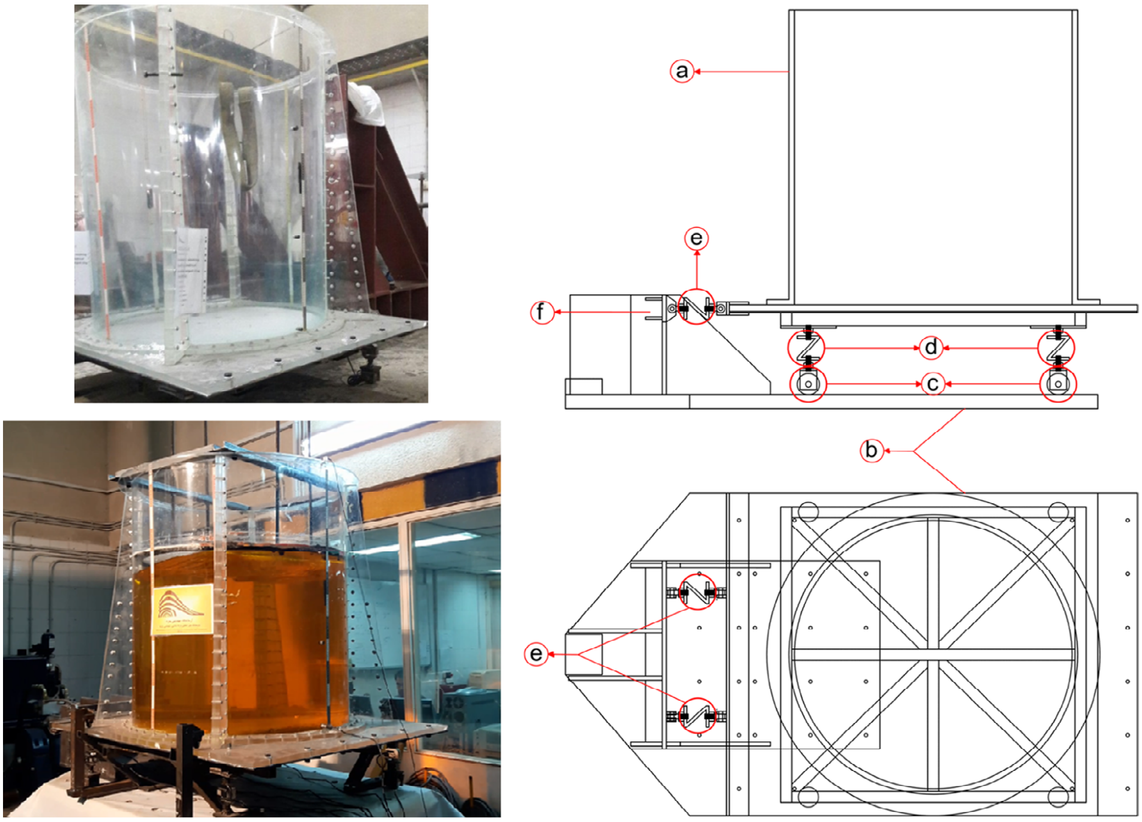


(a) Storage Tank
(b) Shaking Table Base
(c) Bearings under the Tank to Isolate the Tank and Table
(d) Vertical Transducers
(e) Horizontal Transducers for Measuring the Total Shear Force
(f) Steel Structure for Transferring the Shaking Table Displacements to the Tank

**Figure 2.** Schematic and real photo of the experimental setup.

**Table 1.** Details of water heights, H/R, harmonic loadings cases, and freeboards used in experimental tests of current study.

| Water Height (cm) | H/R | Load Case 1 | | Load Case 2 | | Load Case 3 | | Load Case 4 | |
|---|---|---|---|---|---|---|---|---|---|
| | | Amplitude (mm) | Frequency (Hz) | Amplitude (mm) | Frequency (Hz) | Amplitude (mm) | Frequency (Hz) | Amplitude (mm) | Frequency (Hz) |
| 25 | 0.5 | 15 | 0.7 | 1 | 0.814 | 6 | 0.9 | 15 | 1 |
| Freeboard (cm) | | 0, 2, 4, 6, 20* | | 0, 2, 4, 6, 20* | | 0, 2, 4, 6, 20* | | 0, 2, 4, 6, 20* | |
| 50 | 1 | 10 | 0.8 | 1 | 0.931 | 6 | 1 | 10 | 1.1 |
| Freeboard (cm) | | 0, 2, 4, 6, 20* | | 0, 2, 4, 6, 8, 20* | | 0, 2, 4, 6, 20* | | 0, 2, 4, 20* | |
| 75 | 1.5 | 8 | 0.85 | 1 | 0.952 | 4 | 1 | 14 | 1.1 |
| Freeboard (cm) | | 0, 2, 4, 6, 8, 20* | | 0, 2, 4, 6, 8, 20* | | 0, 2, 4, 6, 8, 20* | | 0, 2, 4, 6, 8, 20* | |
| 95 | 1.9 | 8 | 0.85 | 1 | 0.955 | 4 | 1 | 14 | 1.1 |
| Freeboard (cm) | | 0, 1, 2, 3, 4, 5, 20* | | 0, 1, 2, 3, 4, 5, 20* | | 0, 1, 2, 4, 20* | | 0, 1, 2, 3, 4, 5, 20* | |

* Represent freeboard of 20 cm that is the adequate value to avoid liquid-roof collision. Amplitude and Frequency stand for the amplitude and frequency of the loading case, respectively.

Overall, 90 number of experimental tests were performed. In order to assess the reliability and stability of the results, we visually inspected the recorded accelerations and forces resulted from shaking table tests (e.g. check does not have any spike or does not triggered or it does not record thoroughly). This validation process was done for all experimental cases. Following this we decided to re-perform the experiment for about 30 numbers of cases to validate the results and if necessary modify the incorrect measured data.

Maximum base shear forces obtained from 90 experimental tests are listed in Table (2). It is worth mentioning that the effect of bodyweight contained the total base shear recorded by two horizontal transducers which must be eliminated. Consequently, we confirm herein that the net base shear induced by the liquid was obtained from the total recorded shear force based on the primary premise that the tank was solid enough to oscillate consistent with the shaking table oscillations.

Figure (3) shows time histories of the resultant base shear forces for four experimental cases with sufficient freeboards in terms of water height of 75 cm (top row) and 95 cm (2nd row) as well as loading frequencies of 1 Hz (left panels) and 0.85 Hz (right panels). Apparent from this figure, in the first few cycles, the maximum base shear forces under the harmonic loads show high amplitude and decrease gradually over time. Finally, after a few number of cycles, the maximum base shear converge to a constant value, as can be seen in Figure (3). Similar attitude is shown by majority of cases, except the ones having frequency of resonance. Regarding aforementioned statement, the maximum base shear value over the last 20 seconds of the forced vibration of the corresponding time history is considered as the maximum base shear force for almost all cases. Whereas, for the case of resonance with sufficient freeboard, the maximum value of base shear should be considered over the whole loading duration.

From Table (2), it is immediately apparent from the experimental results of the low-frequency loads that the maximum base shear force does not necessarily increase with decreasing freeboard. This observation was contrary to the experimental results obtained from seismic loading discussed

**Table 2.** Maximum base shear force for experimental cases (N).

| H/R | Load | | Freeboard (cm) | | | | | | |
|---|---|---|---|---|---|---|---|---|---|
| 0.5 | Frequency (Hz) | Amplitude (mm) | 0 | 2 | 4 | 6 | 20 | - | - |
| | 0.7 | 15 | 45.52 | 81.25 | 112.42 | 140.24 | 150.74 | - | - |
| | 0.814 | 1 | 6.1 | 33.51 | 77.54 | 113.33 | 223.37 | - | - |
| | 0.9 | 6 | 27.83 | 39.69 | 77.62 | 101.04 | 146.9 | - | - |
| | 1 | 15 | 120.35 | 28.05 | 88.11 | 125.6 | 131.12 | - | - |
| 1 | Frequency (Hz) | Amplitude (mm) | 0 | 2 | 4 | 6 | 8 | 20 | - |
| | 0.8 | 10 | 78.86 | 145.57 | 184.55 | - | - | 218.11 | - |
| | 0.932 | 1 | 14.26 | 52.59 | 114.88 | 172.45 | 192.9 | 308.05 | - |
| | 1 | 6 | 72.76 | 68.77 | 103.73 | 133.68 | - | 185.35 | - |
| | 1.1 | 10 | 152.02 | 54.48 | 66.27 | - | - | 119.98 | - |
| 1.5 | Frequency (Hz) | Amplitude (mm) | 0 | 2 | 4 | 6 | 8 | 20 | - |
| | 0.85 | 8 | 130.91 | 195.28 | 239.7 | 286.11 | 302.62 | 374.1 | - |
| | 0.952 | 1 | 18.14 | 33.94 | 83.12 | 132.48 | 170.73 | 266.88 | - |
| | 1 | 4 | 82.36 | 44.64 | 73.28 | 125.14 | 135.85 | 200.44 | - |
| | 1.1 | 14 | 317.52 | 205.72 | 118.06 | 51.4 | 55.26 | 122.97 | - |
| 1.9 | Frequency (Hz) | Amplitude (mm) | 0 | 1 | 2 | 3 | 4 | 5 | 20 |
| | 0.85 | 8 | 167.1 | 201.93 | 226.42 | 249.15 | 279.89 | 321.5 | 344.92 |
| | 0.955 | 1 | 27.46 | 33.59 | 42.48 | 70.07 | 99.82 | 126.61 | 270.2 |
| | 1 | 4 | 118.62 | 49.87 | 28.17 | - | 26.4 | - | 155.14 |
| | 1.1 | 14 | 437.08 | 314.58 | 273.8 | 218.9 | 202.47 | 154.57 | 63.49 |

* Represent freeboard of 20 cm which is the adequate value to avoid liquid-roof collision.

by Goudarzi et al. [27]. Moreover, according to Table (2), the results show that for harmonic loads with frequency lower or equal to the resonance frequency, the maximum base shear force increases as the freeboard height increases. For harmonic loads with frequencies slightly higher than the resonant frequency, the base shear value increases with decreasing freeboard, which is similar to the observations under seismic loading. Also there is a transition zone that refers to the frequency between resonant frequency and slightly more the results indicate that base shear force might initially decreases and then increase by increasing freeboard (see Figures 4 to 8)

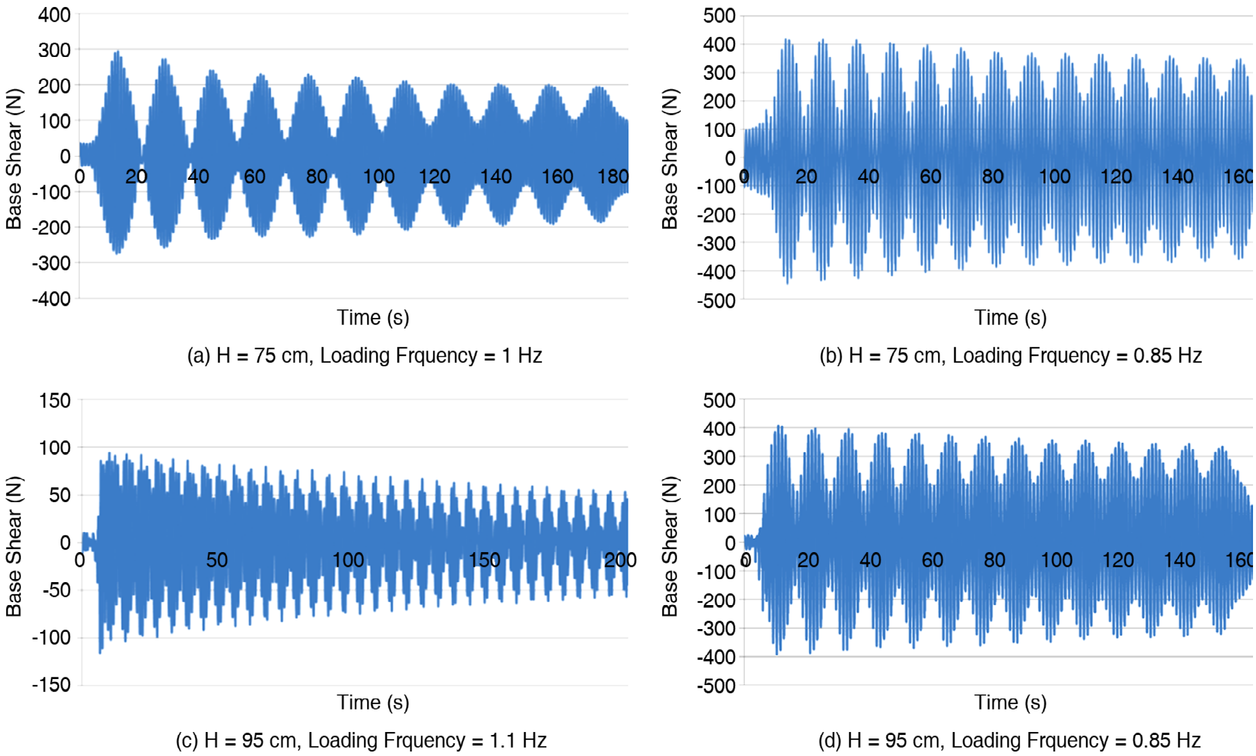


**Figure 3.** Time history of base shear (N) for four experimental cases with sufficient freeboard.

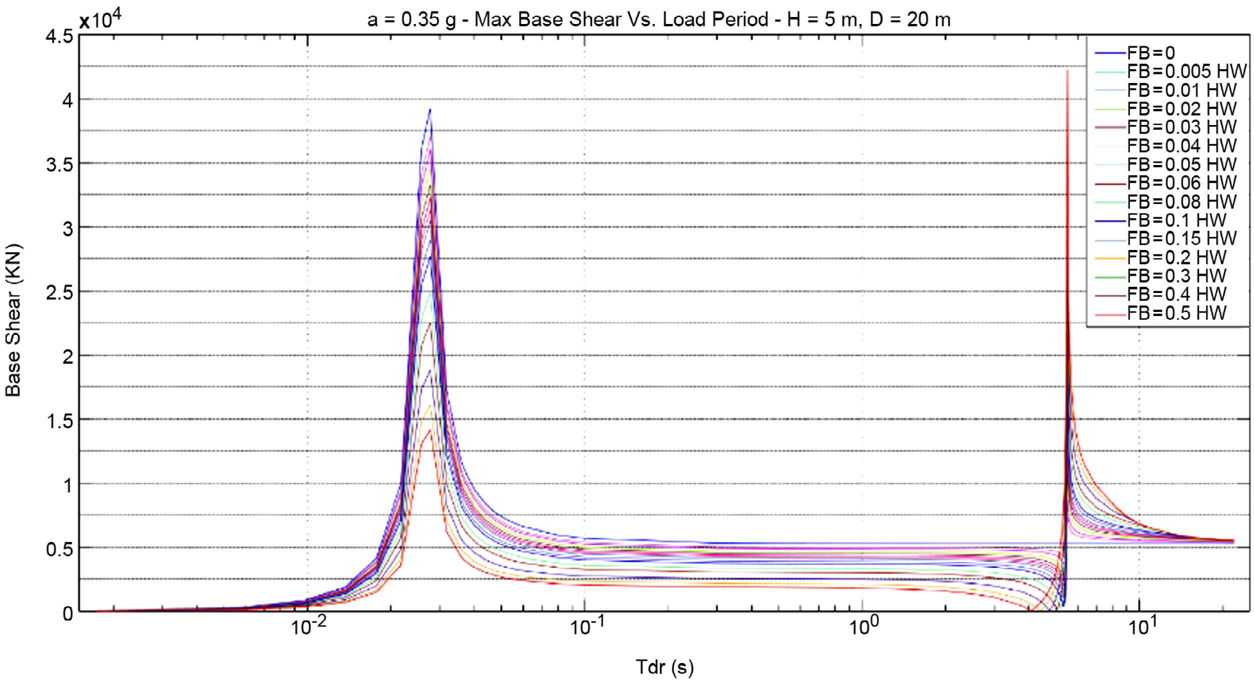


**Figure 4.** MBSF against loading periods (Tdr) for a tank with H/D = 0.25.

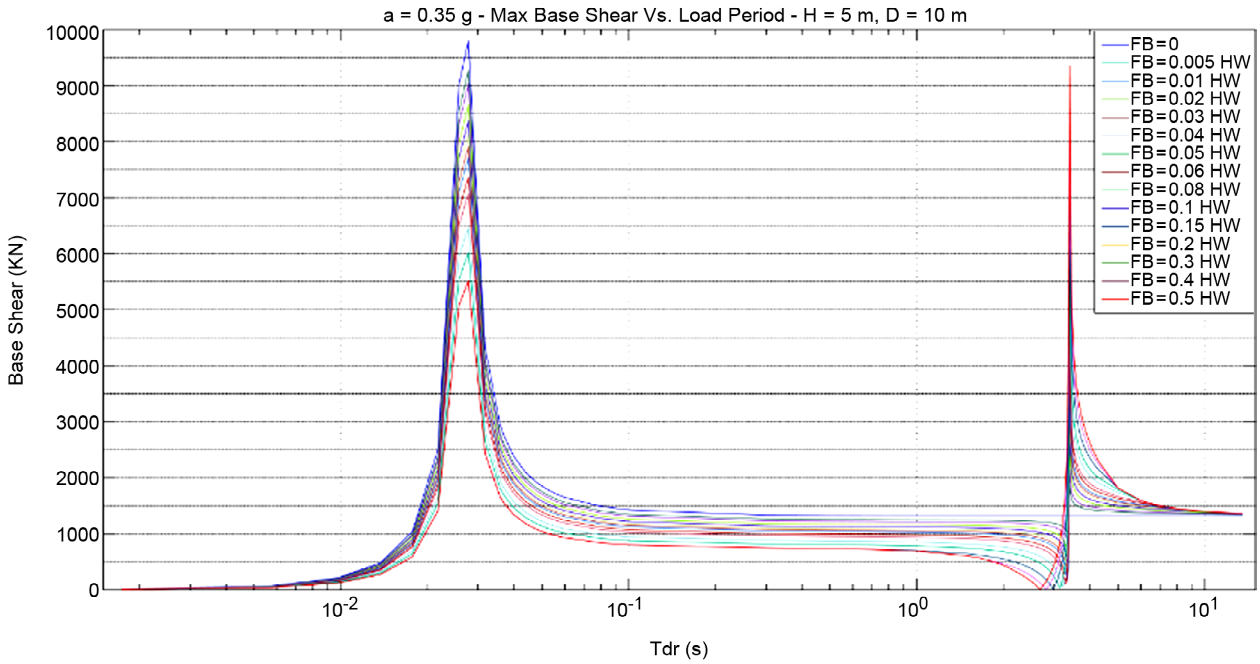


**Figure 5.** MBSF against loading periods (Tdr) for a tank with H/D = 0.5.

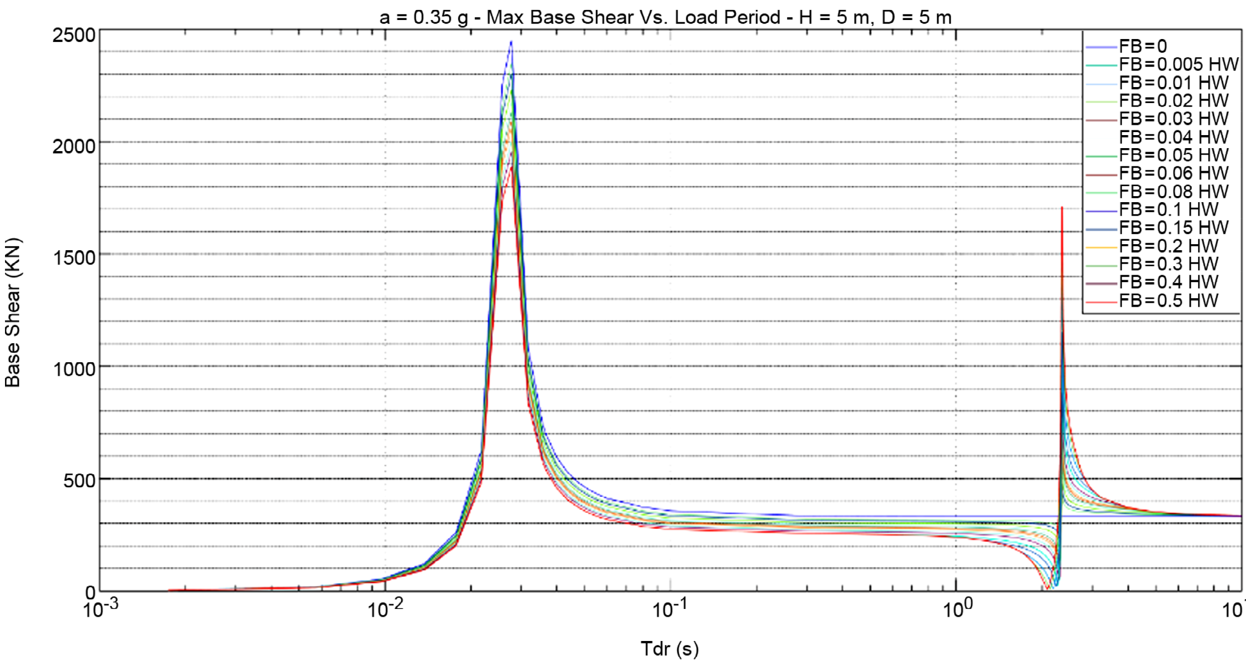


**Figure 6.** MBSF against loading periods (Tdr) for a tank with H/D = 1.

## 4. The Proposed Analytical Technique

As discussed in previous section, the experimental results corroborate the issue that the base shear force under the influence of insufficient freeboard in tanks resulted in a nonlinear trend. Therefore, in order to modify the MSM according to the corresponding insufficient freeboard in tanks, the simplified mechanism of liquid impact on roof should be investigated in detail. Figure (9) depicts the schematic plot of the liquid motion in cylindrical tanks with and without sufficient freeboard. Apparent from left panel of Figure (9), the liquid motion will not collide with the roof for a tank with sufficient freeboard. While, for a tank with insufficient freeboard (Figure 9b), the $A_1$ area on the roof gets wet because of the redistribution of the liquid caused by its collision with the tank roof. To explain more, in the case of zero freeboard, the entire roof is wet, meaning that $A_1$ is equal to $A$. Therefore, as inferred by Equation (3), the decrease

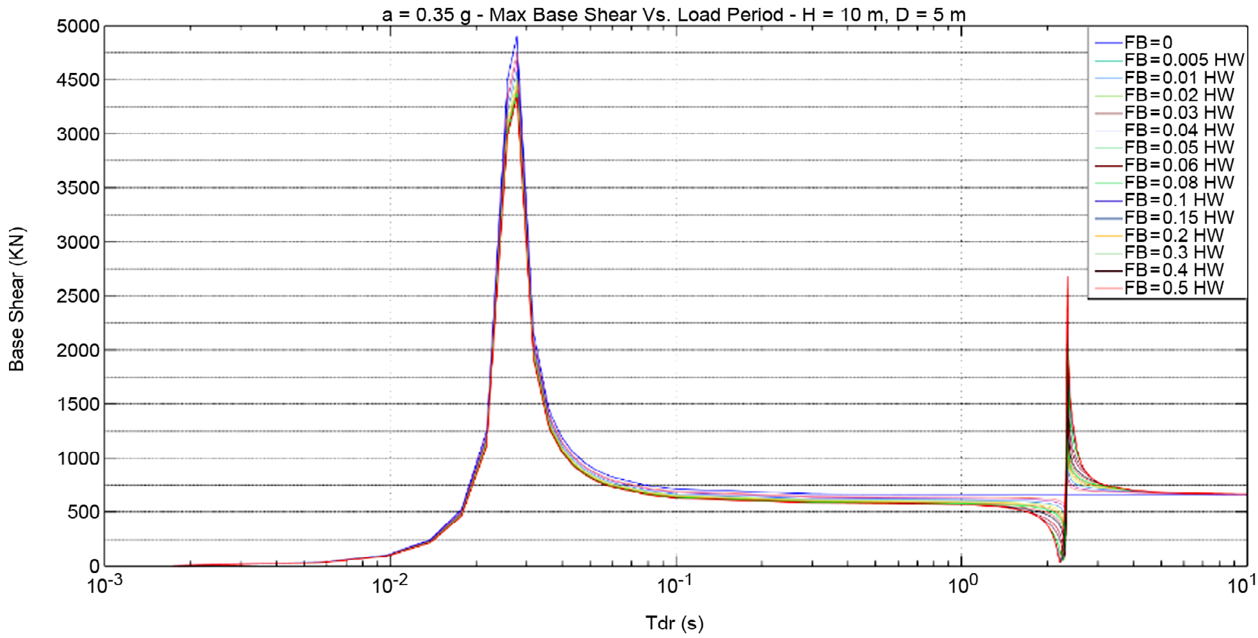


**Figure 7.** MBSF against loading periods (Tdr) for a tank with H/D = 2.

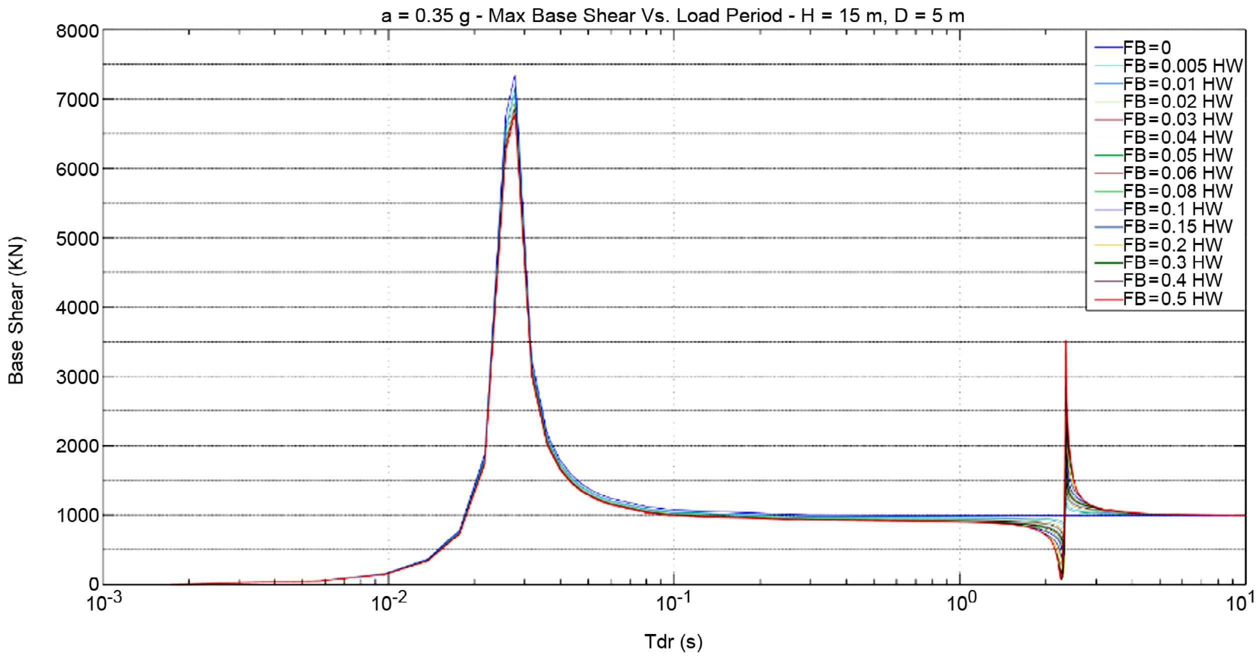


**Figure 8.** MBSF against loading periods (Tdr) for a tank with H/D = 3.

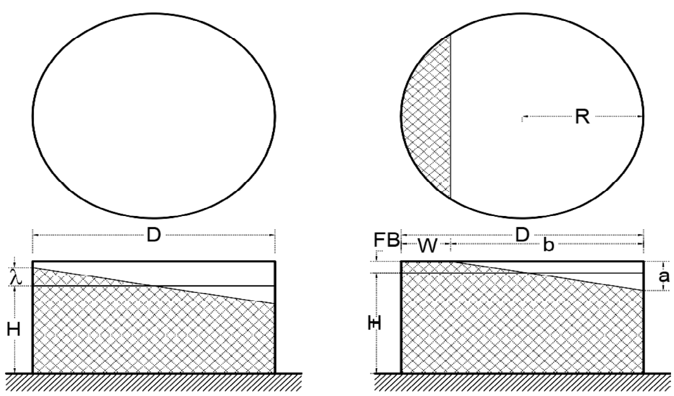


**Figure 9.** Schematic plot of liquid motion in a cylindrical tank.

in convective mass is assumed adversely equivalent to the value of the relative wetted area on the tank roof ($A_1/A$):

$$\frac{A_1}{A}=1-\frac{m_{cm}}{m_{c_{max}}} \tag{3}$$

where $m_{cm}$ is the modified convective mass for insufficient freeboard in a tank and $m_{c_{max}}$ is the original convective mass for the corresponding tank with sufficient freeboard. In other words, having the value of $A_1/A$ enables us to calculate the $m_{cm}$.

As illustrated in Figure (9), at a specific horizontal acceleration, the slope of the free surface liquid for both the sufficient and insufficient freeboard conditions is given by:

$$\frac{R}{\lambda}=\frac{b}{a} \tag{4}$$

Equation (5) is determined by assessing the empty space volume before and after storage liquid motion for the insufficient freeboard as follows:

$$\begin{aligned}&\pi R^2.(FB)=\\&\int_0^b 2x\frac{\lambda}{R}\sqrt{R^2-(R+x-b)^2}\,dx \qquad for \quad b<R\\&\pi R^2.(FB)=\int_0^w 2x\frac{\lambda}{R}\sqrt{R^2-(R+x-w)^2}\,dx+\\&\pi R\lambda(2\times R-w)-\pi R^2\lambda \qquad for \quad b>R\end{aligned} \tag{5}$$

Please refer to Figure (9b) to have a clearer view of the computational process.

The third relationship proposed for the relative wetted area is given by:

$$\begin{aligned}&\alpha=cos^{-1}\left(1-\frac{b}{R}\right),\quad \frac{A_1}{A}=1-\frac{\alpha-cos\,\alpha\, sin\,\alpha}{\pi}\\&\qquad\qquad for \quad b<R\\&\beta=cos^{-1}\left(1-\frac{w}{R}\right),\quad \frac{A_1}{A}=\frac{\beta-cos\,\beta\, sin\,\beta}{\pi}\\&\qquad\qquad for \quad b>R\end{aligned} \tag{6}$$

The following relationship developed from the combination of Equations (4) and (6) for the relative wetted area:

$$\frac{A_1}{A}=1-1.2\left(\frac{FB}{\lambda}\right)^{0.56}+0.2\left(\frac{FB}{\lambda}\right)^{2.22} \tag{7}$$

Using Equation (8), we determine the relative portion of the modified convective mass for a tank with the assumption of insufficient freeboard:

$$\frac{m_{cm}}{m_{c_{max}}}=1.2\left(\frac{FB}{\lambda}\right)^{0.56}-0.2\left(\frac{FB}{\lambda}\right)^{2.22} \tag{8}$$

In Equation (8), $m_{c_{max}}$ represents the original convective mass for the tank with sufficient freeboard, and $\lambda$ is the maximum wave height in tanks without any roof. Both of these values were suggested by the design standard codes (e.g. ACI350). $m_{cm}$ is the modified convective mass in case of insufficient freeboard, and FB is the insufficient freeboard ranging from zero to $\lambda$.

Having $m_{c_{max}}$ and $m_{cm}$ variables, the modified impulsive mass, denoted as $m_{im}$, is calculated using the modified convective mass for the insufficient freeboard through Equation (9) as follows:

$$m_{im}=m_{i_{min}}+m_{c_{max}}-m_{cm} \tag{9}$$

where $m_{i_{min}}$ is the original impulsive mass for a tank with sufficient freeboard.

## 5. Numerical Analysis

As mentioned in previous sections, the use of MSM for assessment of the seismic design parameters of tanks is practical. Goudarzi and Sabbagh-Yazdi [10] examined the accuracy of the MSM numerically, and concluded that this method is capable of precise estimation of the base shear force in tanks with sufficient freeboard. In this section, we aim to evaluate the accuracy of Equations (8) and (9) in tanks with insufficient freeboard compared to the experimental harmonic loading test.

According to these equations, under the circumstance of sufficient freeboard, the impulsive and convective masses are consistent with the mass values given by seismic design standards for tanks. On the other hand, in case of zero freeboard, the whole liquid mass acts as an impulsive mass; in other words, the convective mass becomes zero.

In this section, to evaluate the accuracy of the proposed equations (Equations 8 and 9), impulsive and convective masses are modified based on the actual freeboard, and other parameters such as natural frequency and damping ratio are calculated according to the experimental results for 90 cases in terms of H/R levels, loading (frequency and amplitude), and freeboards. Afterward, the maximum base shear force is calculated using the exploited numerical method. The results are tabulated in Table (3) for all cases. Apparent from Table (3), in the two limit case of zero freeboard and sufficient freeboard (i.e. 20 cm freeboard case), the numerical outcomes are almost similar to the experimental measurements. It should be noted that for both aforementioned limit cases, the initial values of the convective and impulsive masses were used without implementing any adjustment in the numerical solution. Therefore, our numerical model is developed properly.

In Table (3), the difference between maximum base shear forces obtained from the numerical solution and experimental tests are shown in percentages. As can be seen in this table, there is slight difference between the experimental and numerical results which is considered negligible.

**Table 3.** Maximum base shear force for numerical cases (N).

| H/R | Load | | Free Board (cm) | | | | | | |
|---|---|---|---|---|---|---|---|---|---|
| | Frequency (Hz) | Amplitude (mm) | 0 | 2 | 4 | 6 | 20 | - | - |
| **0.5** | 0.7 | 15 | 47.57 | 89.3 | 117.7 | 143.44 | 155.54 | - | - |
| | | | 4.50% | **9.90%** | 4.69% | 2.28% | 3.18% | - | - |
| | 0.814 | 1 | 5.58 | 32.2 | 71.74 | 108.39 | 214.46 | - | - |
| | | | **8.52%** | 3.91% | 7.48% | 4.35% | 3.99% | - | - |
| | 0.9 | 6 | 30.84 | 41.15 | 72.33 | 105.99 | 149.98 | - | - |
| | | | **10.81%** | 3.67% | 6.81% | 4.89% | 2.10% | - | - |
| | 1 | 15 | 111.47 | 25.56 | 86.34 | 120.23 | 134.9 | - | - |
| | | | 7.37% | **8.87%** | 2.01% | 4.27% | 2.88% | - | - |
| | Frequency (Hz) | Amplitude (mm) | 0 | 2 | 4 | 6 | 8 | 20 | - |
| **1** | 0.8 | 10 | 78.54 | 154.97 | 193.13 | - | - | 228.51 | - |
| | | | 0.40% | **6.45%** | 4.65% | - | - | 4.77% | - |
| | 0.932 | 1 | 13.17 | 48.45 | 105 | 177.05 | 197.72 | 297.43 | - |
| | | | 7.64% | 7.87% | **8.60%** | 2.67% | 2.50% | 3.45% | - |
| | 1 | 6 | 74.63 | 65.98 | 101.94 | 131.69 | - | 189.9 | - |
| | | | 2.57% | **4.06%** | 1.72% | 1.49% | - | 2.45% | - |
| | 1.1 | 10 | 154.77 | 46.25 | 63.66 | - | - | 122.13 | - |
| | | | 1.81% | **15.11%** | 3.94% | - | - | 1.79% | - |
| | Frequency (Hz) | Amplitude (mm) | 0 | 2 | 4 | 6 | 8 | 20 | - |
| **1.5** | 0.85 | 8 | 123.67 | 188.66 | 247.16 | 284.17 | 291.76 | 385.59 | - |
| | | | **5.53%** | 3.39% | 3.11% | 0.67% | 3.59% | 3.07% | - |
| | 0.952 | 1 | 17.6 | 33.22 | 78.01 | 126.25 | 172.92 | 273.66 | - |
| | | | 2.97% | 2.12% | **6.15%** | 4.70% | 1.28% | 2.87% | - |
| | 1 | 4 | 82.98 | 42.67 | 71.01 | 118.16 | 134.48 | 190.47 | - |
| | | | 0.75% | 4.41% | 3.10% | **5.58%** | 1.01% | 4.97% | - |
| | 1.1 | 14 | 314.02 | 207.64 | 115.76 | 54.47 | 51.79 | 115.08 | - |
| | | | 1.10% | 0.93% | 1.94% | 5.97% | 6.28% | **6.41%** | - |
| | Frequency (Hz) | Amplitude (mm) | 0 | 1 | 2 | 3 | 4 | 5 | 20 |
| **1.9** | 0.85 | 8 | 159.04 | 198.3 | 220.89 | 244.34 | 263.47 | 296.7 | 338.17 |
| | | | 4.82% | 1.79% | 2.44% | 1.93% | 5.86% | **7.71%** | 1.95% |
| | 0.955 | 1 | 27 | 31.84 | 42.49 | 65.08 | 98.84 | 120.2 | 278.58 |
| | | | 1.67% | 5.20% | 0.02% | **7.12%** | 0.98% | 5.06% | 3.10% |
| | 1 | 4 | 112.24 | 45.48 | 28.46 | - | 24.04 | - | 152.86 |
| | | | 5.38% | 8.80% | 1.03% | - | **8.94%** | - | 1.47% |
| | 1.1 | 14 | 431.97 | 302.71 | 251.07 | 217.94 | 192.7 | 159.06 | 60.28 |
| | | | 1.17% | 3.77% | **8.30%** | 0.43% | 4.82% | 2.90% | 5.05% |

The maximum reported difference is 15.11% which is for H/R = 1, 2 cm freeboard, and load 1.1 Hz and 10 mm amplitude case. Accordingly, we assure that proposed Equations (8) and (9) are proper tools for modifying convective and impulsive masses towards determination of the maximum base shear forces.

Particular attention was paid to comparing the experimental and numerical results to identify any significant bias. For this purpose, as illustrated in Figures (10) and (11), the experimental- and numerical-based time histories of base shear force are plotted against two H/R ratios and load cases for four freeboard heights. No significant bias can be appreciated from 16 cases plotted in Figures (5) and (6).

Generally, we conclude that Equations (8) and (9) are reliable models to modify masses towards

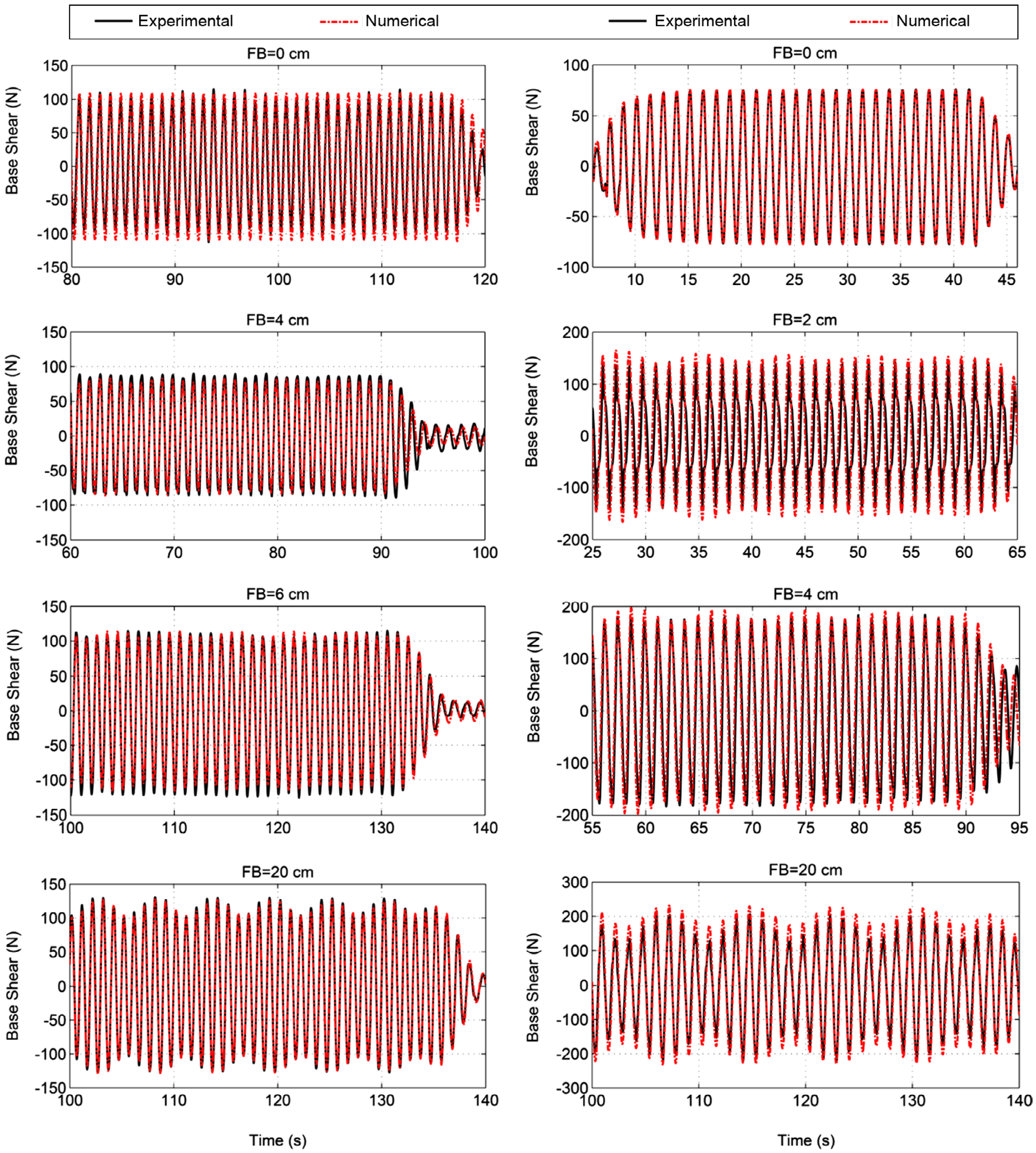


(a) H/R= 0.5, Frequency = 1 Hz, Amplitude = 15 mm

(b) H/R= 1, Frequency = 0.8 Hz, Amplitude = 10 mm

**Figure 10.** Time history of base shear based on a modified MSM and experimental measurements for four freeboard heights. FB stands for freeboard.

designing tanks with insufficient freeboard using the MSM. Similar results were observed when plotting the experimental and numerical base shear time histories for the rest of cases, not shown here for brevity.

### 5.1. Freeboard Effect on Base Shear under Harmonic Load with Different Frequencies

In this section, we studied the effect of freeboard on Maximum Base Shear Force (MBSF) for vertical cylindrical tanks with insufficient freeboard under various harmonic loads. For this purpose, five tanks with H/D ratio of 0.25, 0.5, 1, 2 and 3 and fifteen freeboard heights (FB) from zero to 0.5*H are analyzed in this section. The period range of harmonic loading was selected in a way that it contains both impulsive and convective natural periods ranging from 0.001 to 20 second. The details of diameter (D), liquid height (H) and freeboard height (FB) are shown in Table (4).

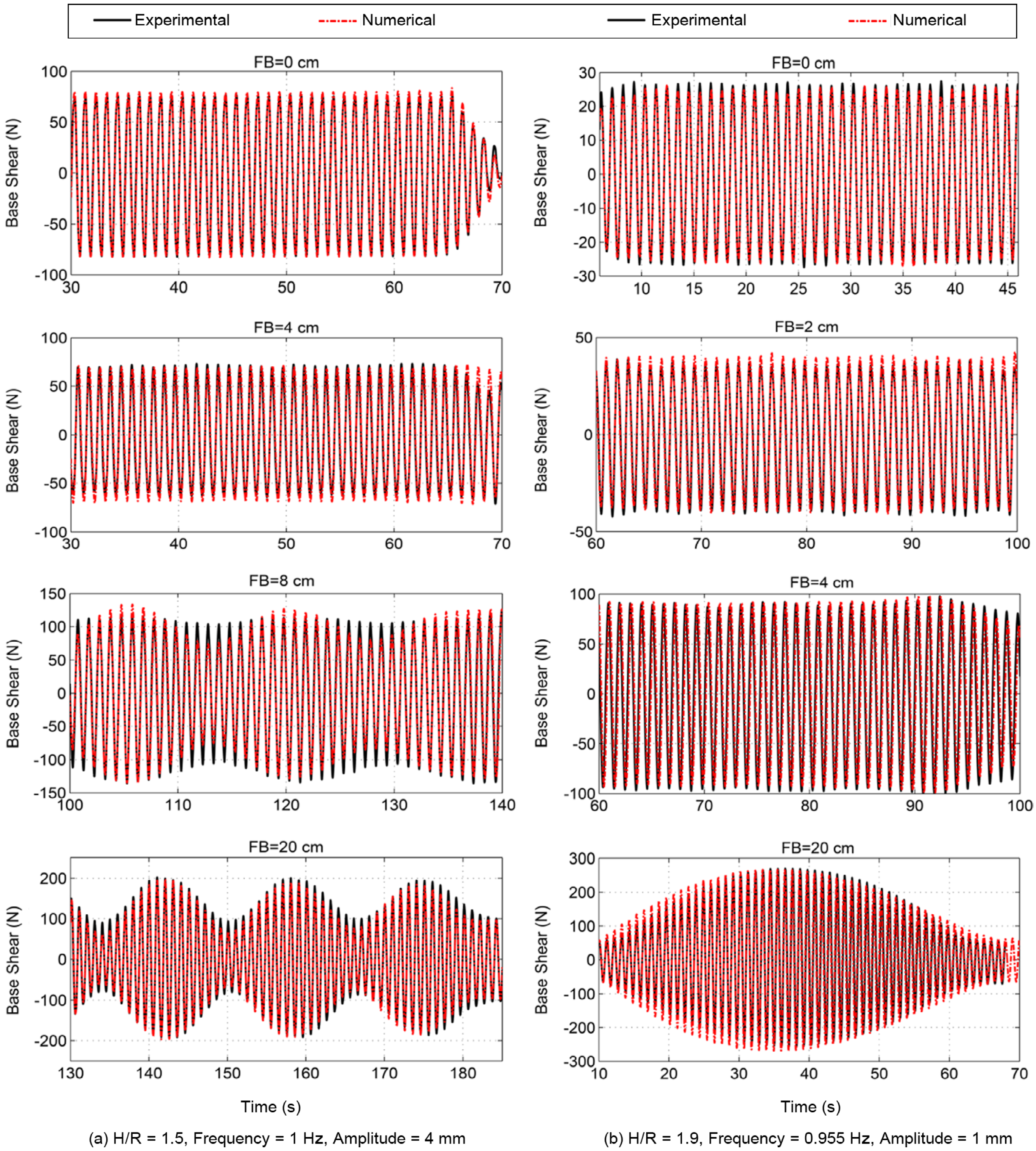


**Figure 11.** Time history of base shear based on a modified MSM and experimental measurements for four freeboard heights. FB stands for freeboard.

**Table 4.** Tanks size and freeboards used in this section.

| H (m) | D (m) | Actual Freeboard |
|---|---|---|
| 5 | 20 | 0 , 0.005*H, 0.01*H, |
| 5 | 10 | 0.02*H, 0.03*H, 0.04*H, |
| 5 | 5 | 0.05*H, 0.06*H, 0.08*H, |
| 10 | 5 | 0.1*H, 0.15*H, 0.2*H, |
| 15 | 5 | 0.3*H, 0.4*H, 0.5*H |

Note D and H stand for diameter and liquid level, respectively.

The maximum wave height was calculated using Equation (10). Note that if the wave height was bigger than the actual freeboard, the masses were modified using Equations (8) and (9).

$$d_{max} = 0.84 * R * \frac{a_c}{g} \quad (10)$$

where $R$, $a_c$ and $g$ are tank's radius, convective mass acceleration and gravitational constant in m/s$^2$ unit, respectively. The results of this section are indicated in Figures (4) to (8) for five different $H/D$. In these figures, the horizontal axis shows loading period (Tdr) in logarithmic unit and the vertical axis is MBSF presented in kN unit. Each figure indicates fifteen freeboard heights plotted by different colors as shown in the legend.

According to these figures, there is considerable evidence that with decreasing the freeboard, the MBSF increases in short-period loads (such as seismic loads). We highlight that the rate of the increasing is higher in broad tank. For instance, in the $T = 0.1$ s, the MBSF for a tank with $H/D = 0.25$, representing broad tanks, and $FB = 0$ is 569.7 kN; however, the MBSF for this tank with $FB = 0.5$*H falls to 205.9 kN, which shows 64% decrease. In the other hand, the MBSF for a tank with $H/D = 3$, representing slender tank, considering the same condition as previous case, the MBSF value falls from 1068 kN to 986 kN, which shows only 7.6% decrease. This emphasizes the significant importance of considering insufficient freeboard in broad tanks.

Apparently, Figures (4) to (8) indicate that unlike short periods, at periods close to the natural period of convective part to longer periods, the MBSF values decrease as FB decreases. Furthermore, the decreasing ratio is higher for broad tanks. As an example, in a tank with $H/D = 0.25$, the MBSF increased almost eight times in the resonance case for $FB = 0.5*H$ compared to $FB = 0$. However, in a slender tank with $H/D = 3$, in the resonance circumstances, the MBSF value increased approximately 3.5 times for $FB = 0.5*H$ than zero freeboard. The reason for reverse MBSF behavior in terms of periods stems from the acceleration of the masses. To elaborate, at short periods, the net acceleration imposed to the impulsive mass is larger than the convective mass. Therefore, when the $FB$ is not adequate, the convective mass subjected to the lower acceleration decreases and the impulsive mass subjected to higher acceleration increases, therefore the total MBSF will increase.

On the other hand, at long periods, ranging from the periods close to the convective resonance period and longer, convective mass is under the higher acceleration and consequently, the total MBSF will decrease due to insufficient freeboard.

As inferred from Figure (10), another fact must be considered is that the MBSF values might be higher at periods longer than seismic periods. Therefore, it is not recommended to design broad tanks subjected to long-period loads based on the mere maximum shear force caused by seismic design loads.

To scrutinize the effect of liquid height, two cylindrical tanks with a fixed roof are studied herein with respect to various loading periods from short to long periods. Tanks with diameters of 20 m and 5 m and maximum heights of 5 m and 15 m, respectively were modeled. After that, we analyzed and determined MBSF changing the height of contained liquid from zero to maximum height of tank in 5 cm steps, for both tanks. Note that we modified the masses using Equations (8) and (9) for cases showing wave sloshing height higher than the actual freeboard. The results of these analyses for short and long periods are illustrated in Figures (12) and (13) for a tank with 15 m diameter and in Figures (14) and (15) for a tank with 5 m diameter. In these figures, the horizontal axis shows liquid height (m), and the vertical axis is MBSF (kN).

According to Figures (13) and (15) indicating short-period MBSFs, it is determined that MBSF occurs when the tank is full. For this reason, for seismic design of tanks during their operational period, the maximum liquid height must be taken into consideration. However, as shown in

Figures (12) and (14) indicating long-period MBSFs, it is apparent that in tanks subjected to long period loads such as the tanks installed in ships or high elevated tanks, the worst case scenario can occur in not thoroughly full tanks. In such conditions, designing tanks based on the maximum elevation of contained liquid may underestimate the MBSF values.

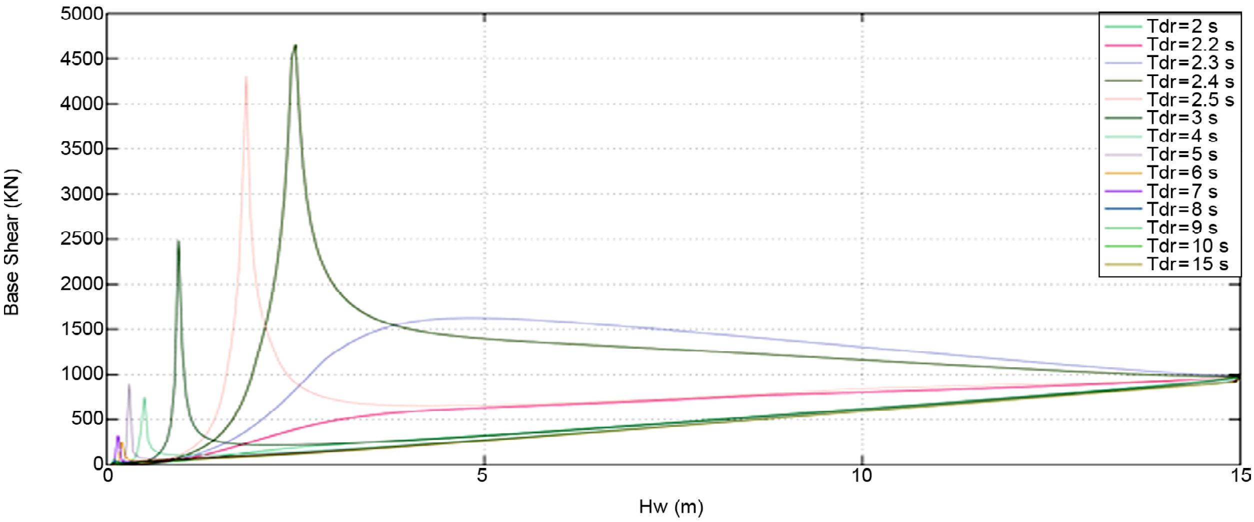


**Figure 12.** MBSF against liquid height (Hw) in a tank with D = 15 m subject to long-period loads.

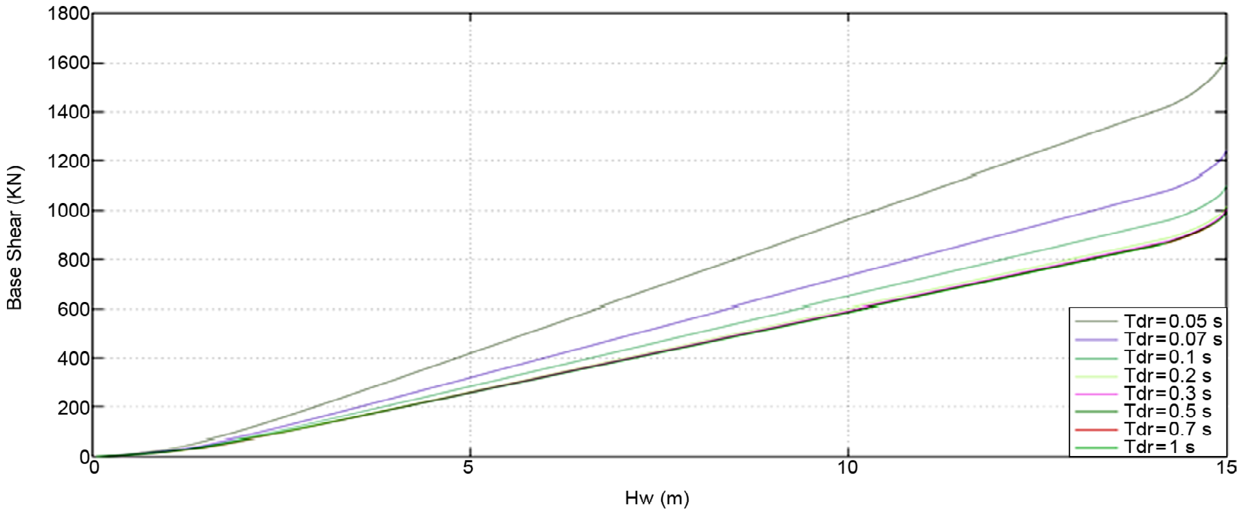


**Figure 13.** MBSF against liquid height (Hw) in a tank with D = 15 m subject to short-period loads.

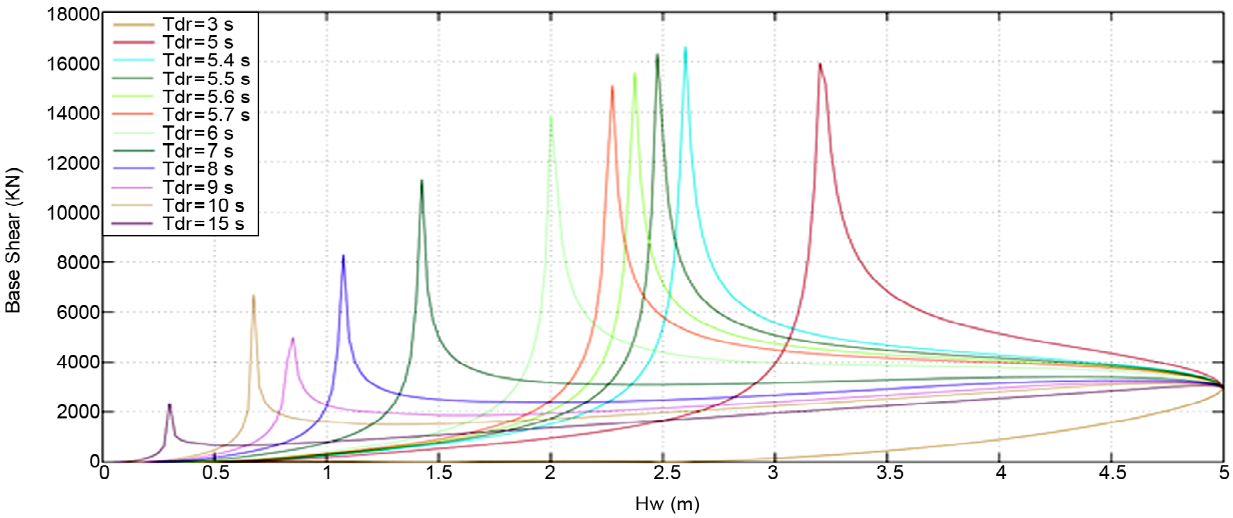


**Figure 14.** MBSF against liquid height (Hw) in a tank with D = 5 m subject to long-period loads.

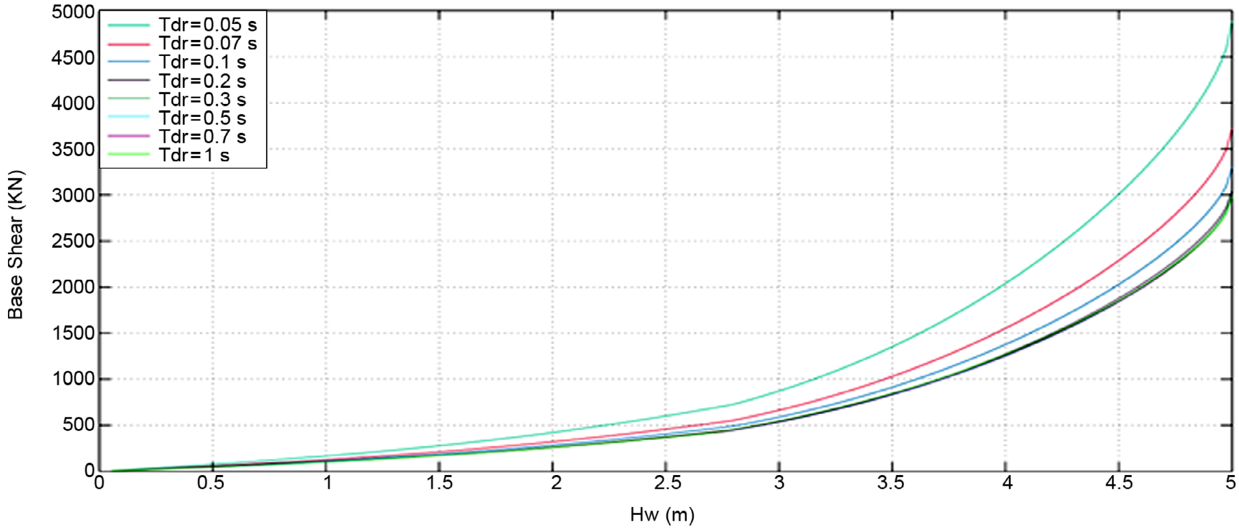


**Figure 15.** MBSF against liquid height (Hw) in a tank with D=5m subject to short-period loads.

## 6. Conclusions

In this study, the sloshing effect in design parameters of cylindrical liquid fixed-roof tanks with insufficient freeboard has been investigated in detail. In this regard, several experimental tests were conducted in the structural laboratory of the International Institute of Earthquake Engineering and Seismology. A total number of 90 experimental tests were performed on a shaking table under several harmonic loads, and their outcomes were derived in terms of total base shear force to explore how dynamic forces change as to the tank roof collision. In these tests, various parametric examinations on contained liquid heights, $H/R$ ratios and freeboards as well as their effects on base shear values were studied elaborately. We observed that despite low-frequency loading condition, the sufficient freeboard reduces the base shear values in high-frequency loads. Furthermore, we conclude that the variation of convective and impulsive masses due to the insufficient freeboard is not linear.

Based on the experimental results, we proposed models to modify the impulsive and convective masses of cylindrical tanks with insufficient freeboard through extensive numerical analyzes performed in current study using the simplified mass spring models for a tank with sufficient freeboard (or a tank without a roof). After that, the effect of loading frequency and liquid height in cylindrical tanks were studied using the modified masses.

We indicated that in broad tanks subjected to the low-frequency loads the MBSF values are higher than those subjected to the high-frequency loads. Furthermore, we proved that in cylindrical tanks subjected to low-frequency loads such as the tanks installed in ships or high elevated tanks, designing tanks based on the maximum elevation of contained liquid may underestimate the MBSF values.

## References

1. Hatayama, K., Zama, S., Nishi, H., Yamada, M., Hirokawa, M., and Inoue, R. (2005) The damages of oil storage tanks during the 2003 Tokachi-oki earthquake and the long period ground motions. In: *Proceedings of the JSCE-AIJ Joint Symposium on Huge Subduction Earthquakes-Wide Area Strong Ground Motion Prediction*, 7-18 (in Japanese).

2. Goudarzi, M.A., Sabbagh-Yazdi, S.R., and Marx, W. (2006) Seismic analysis of hydrodynamic sloshing force on storage tank roof. *Journal of Earthquake Spectra*, **26**, 131-152.

3. Housner, G.W. (1954) *Earthquake Pressures on Fluid Containers*. Eighth Technical Report under Office of Naval Research, Project Designation No. 081-095, California Institute of Technology, Pasadena, California.

4. Housner, G.W. (1957) Dynamic pressures on accelerated fluid containers. *Bulletin of the Seismological Society of America*, **47**(1), 15-35.

5. Housner, G.W. (1963) The dynamic behavior of water tanks. *Bulletin of the Seismological*

*Society of America*, **53**(2), 381-389.

6. Veletsos, A.S. and Yang, J.Y. (1977) Earthquake response of liquid storage tanks advances in civil engineering through mechanics. *In Proceedings of the Second Engineering Mechanics Specialty Conference*, 1-24, Raleigh (NC): ASCE.

7. Haroun, M.A. and Housner, G.W. (1981) Earthquake response of deformable liquid storage tanks. *Journal of Applied Mechanics*, **48**(2), 411-418.

8. Veletsos, A.S. (1984) Seismic response and design of liquid storage tanks: Guidelines for the seismic design of oil and gas pipeline systems. *In Technical Council on Lifeline Earthquake Engineering*, 255-370, New York: ASCE.

9. Malhotra, P.K., Wenk, T., and Wieland, M. (2000) Simple procedures for seismic analysis of liquid storage tanks. *Structural Engineering International, IABSE*, **10**(3), 197-201.

10. Goudarzi, M.A. and Sabbagh-Yazdi, S.R. (2009) Numerical investigation on accuracy of mass spring models for cylindrical tanks under seismic excitation. *Int. J. of Civil Eng.*, **7**, 190-202.

11. Abramson, H.N. (1966) *The Dynamic Behaviour of Liquid in Moving Containers*. Reports SP 106 of NASA.

12. Chen, B.F. and Chiang, H.W. (2000) Complete two-dimensional analysis of sea-wave- induced fully non-linear sloshing fluid in a rigid floating tank. *Journal of Ocean Engineering*, **27**, 953-977.

13. Wu, G.X., Eatock Taylor, R., and Greaves, D.M. (2001) The effect of viscosity on the transient free-surface waves in a two-dimensional tank. *Journal of Engineering Mathematics*, **40**, 77-90.

14. Goudarzi, M.A. and Sabbagh-Yazdi, S.R. (2012) Investigation of nonlinear sloshing effects in seismically excited tanks. *Soil Dynamics and Earthquake Engineering*, **43**, 355-365.

15. Kabiri, M.M., Nikoomanesh, M.R., Nouraei Danesh, P., and Goudarzi, M.A. (2019) Numerical and experimental evaluation of sloshing wave force caused by dynamic loads in liquid tanks. *Journal of Fluids Engineering*, FE-19-1029.

16. De Angelis, M., Giannini, R., and Paolacci, F. (2010) Experimental investigation on the seismic response of a steel liquid storage tank equipped with floating roof by shaking table tests. *Earthquake Engineering and Structural Dynamics*, 39(4), 377-396.

17. Zhang, R., Weng, D., and Ge, Q. (2014) Shaking table experiment on a steel storage tank with multiple friction pendulum bearings. *Structural Engineering and Mechanics*, **52**(5), 875-887.

18. Burkacki, D. and Jankowski, R. (2014) Experimental study on steel tank model using shaking table. *Civil and Environmental Engineering Reports, CEER 2014*, **14**(3), 37-47.

19. Bae, D. and Park, J.H. (2018) Shaking table test of steel cylindrical liquid storage tank considering the Roof Characteristics. *International Journal of Steel Structures*, **18**(4), 1167-1176.

20. Park, J.H., Bae, D., and Oh, C.K. (2016) Experimental study on the dynamic behavior of a cylindrical liquid storage tank subjected to seismic excitation. *International Journal of Steel Structures*, **16**, 935-945.

21. Milgram, J.H. (1969) The motion of a fluid in a cylindrical container with a free surface following vertical impact. *Journal of Fluid Mechanics*, **37**(3), 435-448.

22. Minowa, C. (1997) Sloshing impact of a rectangular water tank (water tank damage caused by the Kobe Earthquake). *Nippon Kikai Gakkai Ronbunshu Chen*, **63**(612), 2643-2649.

23. Minowa, C., Ogawa, N., Harada, I., and Ma, D.C. (1994) *Sloshing Roof Impact Tests of a Rectangular Tank (ANL/RE/CP-82360; CONF-940613-13)*. Argonne National Lab., IL., United States.

24. Goudarzi, M.A., Sabbagh-Yazdi, S.R., and Marx, W. (2010) Seismic analysis of hydrodynamic

sloshing force on storage tank roof. *Journal of Earthquake Spectra*, **26**, 131-152.

25. Malhotra, P.K. (2005) Sloshing loads in liquid-storage tanks with insufficient freeboard. *Earthquake Spectra*, **21**(4), 1185-1192.

26. Malhotra, P.K. (2006) Earthquake induced sloshing in tanks with insufficient freeboard. *Structural Engineering International*, **16**(3), 222-225.

27. Goudarzi, M.A., Moosapoor, M., and Nikoo-manesh, M.R. (2019) Seismic design loads of cylindrical liquid tanks with insufficient free-board. *Earthquake Spectra*, Accepted Paper.